Insulin Stimulates Human Skeletal Muscle Protein Synthesis via an Indirect Mechanism Involving Endothelial-Dependent Vasodilation and Mammalian Target of Rapamycin Complex 1 Signaling

Kyle L. Timmerman, Jessica L. Lee, Hans C. Dreyer, Shaheen Dhanani, Erin L. Glynn, Christopher S. Fry, Micah J. Drummond, Melinda Sheffield-Moore, Blake B. Rasmussen, and Elena Volpi

Sealy Center on Aging (K.L.T., J.L.L., H.C.D., S.D., M.J.D., M.S.-M., B.B.R., E.V.), Departments of Internal Medicine (M.S.-M., E.V.) and Physical Therapy (H.C.D., M.J.D., B.B.R.), and Division of Rehabilitation Sciences (H.C.D., E.L.G., C.S.F., M.J.D., B.B.R.); University of Texas Medical Branch, Galveston, Texas 77555

Objective: Our objective was to determine whether endothelial-dependent vasodilation is an essential mechanism by which insulin stimulates human skeletal muscle protein synthesis and anabolism.

Subjects: Subjects were healthy young adults (n = 14) aged 31 ± 2 yr.

Design: Subjects were studied at baseline and during local leg infusion of insulin alone (control, n = 7) or insulin plus the nitric oxide synthase inhibitor *NG*-monomethyl-L-arginine (L-NMMA, n = 7) to prevent insulin-induced vasodilation.

Methods: We measured skeletal muscle protein metabolism with stable isotope tracers, blood flow with indocyanine green, capillary recruitment with contrast enhanced ultrasound, glucose metabolism with stable isotope tracers, and phosphorylation of proteins associated with insulin (Akt) and amino acid-induced mammalian target of rapamycin (mTOR) complex 1 (mTORC1) signaling (mTOR, S6 kinase 1, and eukaryotic initiation factor 4E-binding protein 1) with Western blot analysis.

Results: No basal differences between groups were detected. During insulin infusion, blood flow and capillary recruitment increased in the control ($P < 0.05$) group only; Akt phosphorylation and glucose uptake increased in both groups ($P < 0.05$), with no group differences; and mTORC1 signaling increased more in control ($P < 0.05$) than in L-NMMA. Phenylalanine net balance increased ($P < 0.05$) in both groups, but with opposite mechanisms: increased protein synthesis (basal, 0.051 ± 0.006 %/h; insulin, 0.077 ± 0.008 %/h; $P < 0.05$) with no change in proteolysis in control and decreased proteolysis ($P < 0.05$) with no change in synthesis (basal, 0.061 ± 0.004 %/h; insulin, 0.050 ± 0.006 %/h; *P* value not significant) in L-NMMA.

Conclusions: Endothelial-dependent vasodilation and the consequent increase in nutritive flow and mTORC1 signaling, rather than Akt signaling, are fundamental mechanisms by which insulin stimulates muscle protein synthesis in humans. Additionally, these data underscore that insulin modulates skeletal muscle proteolysis according to its effects on nutritive flow. **(*J Clin Endocrinol Metab* 95: 3848–3857, 2010)**

ISSN Print 0021-972X ISSN Online 1945-7197
Printed in U.S.A.

doi: 10.1210/jc.2009-2696 Received December 16, 2009. Accepted April 21, 2010.
First Published Online May 19, 2010

Abbreviations: 4E-BP1, Eukaryotic initiation factor 4E-binding protein 1; eNOS, endothelial nitric oxide synthase; FSR, fractional synthesis rate; ICG, indocyanine green; L-NMMA, *NG*-monomethyl-L-arginine; mTOR, mammalian target of rapamycin; mTORC1, mTOR complex 1; PI, pulsing interval; PKB, protein kinase B; S6K1, S6 kinase 1; TSC2, tuberous sclerosis complex 2.

The longstanding debate on whether insulin stimulates skeletal muscle protein synthesis in humans has yet to be settled. Insulin has been reported to stimulate skeletal muscle protein synthesis in animals (1–4) and humans (5, 6). Conversely, some human studies could not demonstrate significant changes in muscle protein synthesis with hyperinsulinemia while reporting an inhibitory effect on proteolysis (7–9). We have hypothesized that these discrepancies may be due to differences in muscle perfusion, nutritive flow, and/or amino acid availability, which then modulate insulin's effect on muscle protein synthesis and breakdown (10–12). However, the fundamental question of how insulin stimulates human skeletal muscle protein synthesis and anabolism remains unanswered.

At the cellular level, insulin induces phosphorylation of Akt/protein kinase B (PKB) and mammalian target of rapamycin (mTOR) with a subsequent increase in the phosphorylation of eukaryotic initiation factor 4E-binding protein 1 (4E-BP1) and p70 ribosomal protein S6 kinase 1 (S6K1). That is, insulin increases mTOR complex 1 (mTORC1) signaling, promoting translation initiation and accelerating muscle protein synthesis (13). Insulin also stimulates endothelial-dependent vasodilation by activating endothelial nitric oxide synthase (eNOS) (14–16), increasing capillary recruitment, microvascular volume, and nutritive flow to skeletal muscle in healthy young adults (17). This increased muscle perfusion raises the amount of muscle tissue exposed to insulin, nutrients, and amino acids, which can increase Akt and mTORC1 signaling, stimulating muscle protein synthesis (10). Conversely, skeletal muscle protein synthesis is resistant to insulin in healthy nondiabetic older subjects, a defect associated with both reduced vasodilation (12) and blunted Akt/mTORC1 signaling, which a single bout of aerobic exercise can reverse (18). In general, the ability of insulin to promote muscle protein synthesis and net deposition correlates positively with muscle blood flow and amino acid delivery in young and older subjects(10–12, 18). Amino acids activate mTORC1 signaling (19), making it very difficult to determine the main mechanism through which insulin stimulates human skeletal muscle protein synthesis, *i.e.* directly, via Akt signaling, or indirectly, via endothelial-dependent vasodilation increasing tissue exposure to insulin and amino acids and, consequently, mTORC1 signaling, or both.

The purpose of the present study was to determine the role of insulin-induced endothelial-dependent vasodilation on the insulin stimulation of muscle protein synthesis and net protein anabolism. We hypothesized that pharmacological inhibition of endothelial-dependent vasodilation would attenuate the stimulatory effect of insulin on skeletal muscle protein synthesis in young healthy subjects. To test this hypothesis, we measured skeletal muscle blood flow, perfusion, anabolic signaling, protein synthesis, and glucose kinetics in young healthy subjects at baseline and during local hyperinsulinemia in one leg. During insulin infusion, one group also received a concomitant infusion of the nitric oxide synthase inhibitor *NG*-monomethyl-L-arginine (L-NMMA) to prevent insulin-induced vasodilation (20).

Subjects and Methods

Ethical approval

After approval by the Institutional Review Board of the University of Texas Medical Branch (Galveston, TX) and the U.S. Food and Drug Administration (IND 73,870), all subjects read and signed a written informed consent form before enrollment.

Subjects (Table 1)

Fourteen young subjects from the Houston/Galveston, TX, area participated in a single acute experiment after random assignment to a control group receiving insulin only or an experimental group receiving insulin plus L-NMMA. All subjects were healthy and had normal glucose tolerance based on clinical history, physical examination, and laboratory tests, including a 2-h 75-g oral glucose tolerance test.

Study design

We measured skeletal muscle blood flow, perfusion, anabolic signaling, protein synthesis, phenylalanine kinetics, and glucose kinetics in the postabsorptive basal state (0–240 min) and during infusion of insulin (240–420 min) alone (control) or with L-NMMA (L-NMMA). Subjects were admitted to the University of Texas Medical Branch Clinical Research Center the afternoon before the experiment. They received a standardized meal at 1900 h (one third of their estimated daily energy requirements) and a snack at 2200 h, after which they were allowed only water until the end of the study (1400 h).

The next morning at 0600 h, polyethylene catheters were inserted into a forearm vein for stable isotope tracers (Isotec Inc., Sigma-Aldrich, Miamisburg, OH) and dextrose infusion, a contralateral hand vein for arterialized blood sampling, and the common femoral artery and vein of one leg for blood sampling. The arterial line was also used for infusion of indocyanine green (ICG) (IC-Green; Akorn, Lake Forest, IL), insulin, and L-NMMA. At 0700 h, we drew a background blood sample for phenylalanine and glucose enrichment and ICG concentration and started (time = 0 min) a primed-continuous infusion of L-[ring-$^{13}C_6$]phenylalanine

TABLE 1. Subjects' characteristics

	Control	L-NMMA
n	7	7
Sex	5 females, 2 males	4 females, 3 males
Age (yr)	32 ± 2	32 ± 3
Weight (kg)	67.7 ± 5.5	70.8 ± 5.8
Height (cm)	1.63 ± 0.04	1.68 ± 0.05
Body mass index (kg/m^2)	25 ± 1	25 ± 1
Leg volume (liters)	9.09 ± 0.6	9.90 ± 0.7

Values are the mean ± SE.

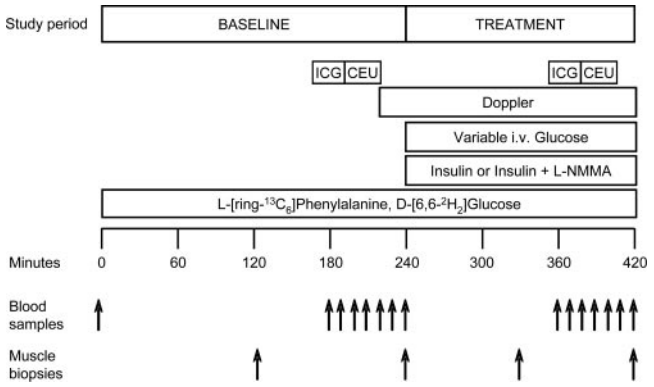

FIG. 1. Study design. Blood and muscle sampling is indicated by *arrows*. A detailed description of the study design is provided in the text.

(prime, 2 μmol/kg; infusion, 0.05 μmol/kg · min) and D-[6,6-$^2H_2$]glucose (prime, 19 μmol/kg; infusion, 0.22 μmol/kg · min), which was maintained until the end of the study (Fig. 1). After 120 min, a first muscle biopsy was taken from the vastus lateralis of the leg bearing the femoral catheters, using aseptic technique, local anesthesia (1% lidocaine), and a 5-mm Bergström needle. The tissue (100–200 mg) was quickly rinsed with ice-cold saline to remove excess blood, blotted gently with a sterile sponge, frozen in liquid nitrogen, and stored at −80 C until analyzed.

At 150 min ICG (0.5 mg/min) was started into the common femoral artery. After 10 min, four sequential blood samples were drawn at 10-min intervals from both femoral vein and hand vein to measure blood flow. At 180 min, after stopping the ICG infusion, we infused perflutren lipid microsphere (Definity; Lantheus Medical Imaging, N.Billerica, MA) in the wrist vein to measure muscle perfusion of the vastus lateralis. Subsequently, four blood samples were drawn at 5-min intervals from the hand vein and femoral vein and artery to determine insulin concentrations as well as phenylalanine and glucose concentrations and enrichments. At 240 min, the second muscle biopsy was taken from the same incision of the first, at a different needle angle.

After the second biopsy, we started an insulin infusion (Novolin R; Novo Nordisk, Princeton, NJ; 0.15 mU/min · 100 ml of leg) in the femoral artery of both groups and continued it until the end of the experiment (420 min). This insulin infusion rate was used to increase leg insulin concentration and availability to the same postprandial levels in both groups, while avoiding hypoaminoacidemia due to systemic hyperinsulinemia (7, 9, 21). Dextrose (20%) enriched 2% with D-[6,6-$^2H_2$]glucose was infused at a variable rate to maintain blood glucose at the basal concentration (hyperinsulinemic-euglycemic clamp). In the L-NMMA group, we also infused L-NMMA at variable rate into the femoral artery to prevent insulin-induced vasodilation based on frequent Doppler measures (Philips ATL Ultrasound, Andover, MA) of the superficial femoral artery. Average L-NMMA infusion rate during the last hour of the experiment was 0.089 ± 0.009 mg/kg · min.

Additional muscle biopsies were taken from a new incision, 5 cm proximal to the first, at 330 and 420 min. Between 360 and 420 min, the blood flow and muscle perfusion measurements were repeated, and blood samples were drawn for tracer enrichment and phenylalanine, glucose, and insulin concentration as described above.

Analytical methods

Plasma glucose concentration was measured using an automated glucose analyzer (Yellow Springs Instrument Co., Yellow Springs, OH). ELISAs were used to determine insulin (Linco, St. Charles, MO) and endothelin-1 (R&D Systems, Inc., Minneapolis, MN) concentrations with a microplate reader (Bio-Rad, Hercules, CA).

Blood flow was measured based on ICG concentration in femoral and wrist veins by spectrophotometrical determination (Beckman Coulter, Fullerton, CA) at $\lambda = 805$ (22).

Muscle perfusion was measured at baseline and during hyperinsulinemia using contrast enhanced ultrasound as described by others (23, 24). Ultrasound imaging of the vastus lateralis muscle was performed in a transaxial plane approximately 15–20 cm above the patella over the midportion of the muscle using a P4-2 phased array transducer. An octafluoropropane gas-filled albumin microbubbles suspension (Definity, St. Louis Park, MN) was infused iv (3.5 ml/min for 8 min), using a mechanical index of 1.3 and compression of 80%. Once the systemic microbubble concentrations reached steady state (~2 min), background images were obtained at a frame rate of 1/sec. Intermittent imaging was performed using an internal timer at pulsing intervals (PI) ranging from 1–25 sec, allowing progressively greater replenishment of the ultrasound beam elevation between destructive pulses. Depth, focus, and gain were optimized at the beginning of each experiment and held constant throughout. Data were recorded on a SVHS tape and digitized for analysis using an offline system. A minimum of three images were acquired at each PI. The background-subtracted video intensity at each PI was measured from a region of interest within the vastus lateralis muscle. PI *vs.* video intensity data were curve fitted to the function $y = A \times (1 - e^{-\beta t})$, where y is the video intensity at PI time t, A is the plateau video intensity (an index of microvascular blood volume), and β is the rate of microvascular refilling (an indicator of microvascular flow velocity) (25).

Total and phosphorylated Akt, tuberous sclerosis complex 2 (TSC2), mTOR, 4E-BP1, and S6K were measured in skeletal muscle samples collected at 120, 330, and 420 min using SDS-PAGE and immunoblotting (Bio-Rad) as previously described (26). Primary antibodies were purchased from Cell Signaling Technology (Beverly, MA). The concentrations and binding sites were as follows: phospho-Akt (Ser473, 1:1000, and Thr308, 1:1000), phospho-TSC2 (Thr1462, 1:500), phospho-mTOR (Ser2448, 1:1000), phospho-4E-BP1 (Thr37/46, 1:1000), and phospho-p70 S6K1 (Thr389, 1:500). Antirabbit IgG horseradish peroxidase-conjugated secondary antibody (Amersham Bioscience, Piscataway, NJ) was used at a concentration of 1:2000. For each protein, total content was detected using an antibody dilution of 1:1000. Both phosphorylated and total proteins were normalized to a rodent internal loading control. Data are expressed as normalized phosphorylated protein.

Muscle tissue was ground, and free amino acids and proteins were extracted as previously described (27). After protein hydrolysis and amino acid purification, mixed muscle protein-bound phenylalanine enrichment was determined using gas chromatography-mass spectrometry (Agilent Technologies, Palo Alto, CA) and the external standard curve approach (27). Blood and intracellular free phenylalanine concentrations and enrichments, and blood glucose enrichments were determined by gas chromatography-mass spectrometry as previously described (27).

Calculations

The fractional synthesis rate (FSR) of mixed muscle proteins was calculated between 120–240 and 240–420 min from the incorporation rate of L-[ring-$^{13}C_6$]phenylalanine into the pro-

teins and the free-tissue phenylalanine enrichment using the precursor-product model: FSR = $\{(\Delta E_p/t)[(E_{M(1)} + E_{M(2)})/2]\}$, where ΔE_P is the increment of protein-bound phenylalanine enrichment between two sequential biopsies, t is the time interval between the two sequential biopsies, and $E_{M(1)}$ and $E_{M(2)}$ are phenylalanine enrichments (tracer/tracee ratio) in the free muscle pool in two subsequent biopsies. Results are presented as percentage per hour.

Muscle phenylalanine kinetics was calculated using two- and three-pool models that provide unique information regarding leg plasma and intracellular phenylalanine kinetics, respectively (28). The parameters include the following: delivery to the leg = $C_A \times$ BF; output from the leg = $C_V \times$ BF; net balance (NB) = $(C_A - C_V) \times$ BF; leg rate of appearance (Ra) = BF $\times$ C_A $[(E_A/E_V) - 1]$; leg rate of disappearance = leg Ra + NB = BF $\times$ $[(C_A - E_A/E_V) - C_V]$; release from proteolysis ($F_{M,0}$) = $\{[(E_M - E_V)/(E_A - E_M) \times C_V] + C_A\} \times [(E_A/E_M) - 1] \times$ BF; and utilization for protein synthesis = $F_{M,0}$ + NB, where C_A and C_V are phenylalanine concentrations in the femoral artery and vein, respectively; E_A, E_V, and E_M are phenylalanine enrichments (tracer to tracee ratio) in the femoral artery, femoral vein, and muscle; and BF is blood flow. Data are expressed as per 100 ml of leg volume.

Basal whole-body endogenous glucose production and utilization were calculated using the single-pool model (27): endogenous glucose production = whole-body glucose utilization = i/GE_A, where GE_A is glucose arterial enrichment and i is tracer infusion rate. During clamp, endogenous glucose production was calculated by subtracting the exogenous glucose infusion rate from whole-body glucose utilization.

Leg glucose utilization was calculated as the product of blood flow by the arteriovenous difference in glucose concentration ($G_A - G_V$): leg glucose utilization = $(G_A - G_V) \times$ BF.

Insulin delivery to the leg was calculated as the product of femoral vein insulin concentration by blood flow.

Statistical analysis

Subjects' characteristics and baseline values for all measured variables were analyzed using one-way ANOVA. To determine the effects of inhibition of insulin-dependent vasodilation, comparisons were performed using ANOVA with repeated measures. The factors were subject, time (basal and insulin), and group (control and L-NMMA). *Post hoc* pairwise multiple comparisons were performed using the Bonferroni *t* test. The level of significance was set at $P < 0.05$ and the trend level at $P < 0.10$. Statistical procedures were performed using SigmaStat 3.5 (Systat Software Inc., San Jose, CA).

Results

No baseline differences were detected between groups for any measured parameters.

Blood flow, muscle perfusion, and endothelin-1 (Fig. 2)

Blood flow and muscle perfusion increased significantly during insulin infusion in the control group only ($P < 0.05$) but did not change in the L-NMMA group.

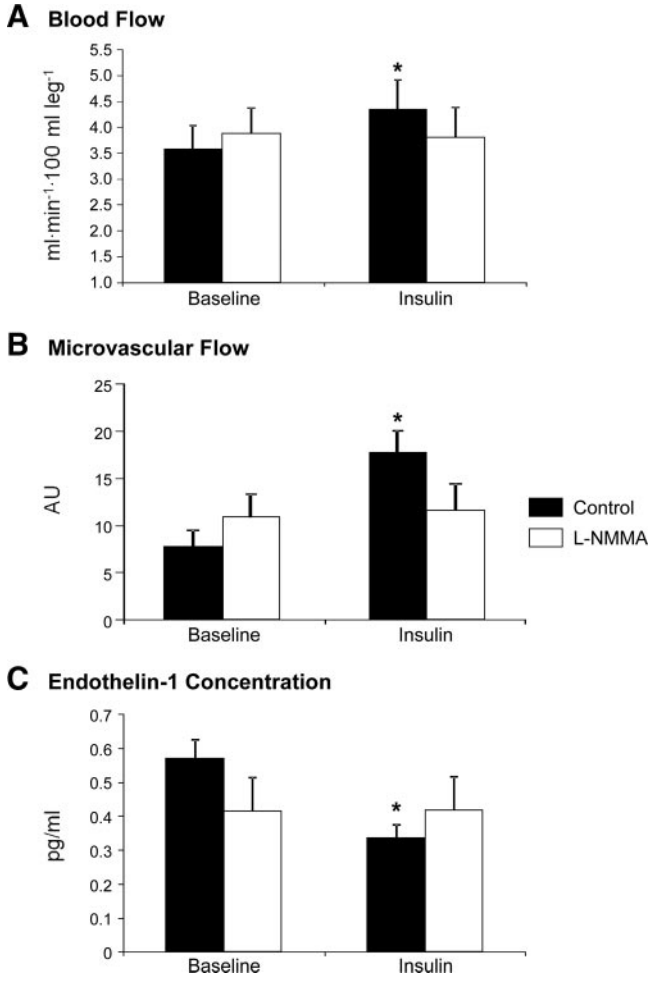

FIG. 2. Leg blood flow by dye dilution (ICG) (A), muscle microvascular flow by contrast enhanced ultrasound (CEU) (B), and endothelin-1 concentrations in the femoral vein (C) in two groups of healthy young subjects at baseline and during local insulin infusion in one leg with (L-NMMA) or without (control) concomitant infusion of the eNOS inhibitor L-NMMA. Data are the mean ± SE. *, $P < 0.05$ *vs.* baseline. AU, Arbitrary units.

Endothelin-1 decreased significantly ($P < 0.05$) with hyperinsulinemia only in the control group and did not change in the L-NMMA group.

Insulin and glucose kinetics (Table 2)

During hyperinsulinemic-euglycemic clamp, arterial glucose concentration did not significantly change in either group, whereas systemic and femoral insulin concentrations, insulin delivery to the leg, and leg and whole-body glucose utilization increased significantly ($P < 0.05$) in both groups with no differences between groups. Endogenous glucose production decreased significantly ($P < 0.05$) in both groups during hyperinsulinemia, with no between-group differences.

Anabolic signaling (Fig. 3)

There were no significant differences in total protein across biopsy times for any proteins measured. During in-

TABLE 2. Insulin and glucose concentrations and kinetics in two groups of healthy young subjects at baseline and during local insulin infusion in one leg with (L-NMMA) or without (control) concomitant infusion of the eNOS inhibitor L-NMMA

	Control		L-NMMA	
	Baseline	**Insulin**	**Baseline**	**Insulin**
Insulin				
Systemic concentration (pmol/liter)	35 ± 4	65 ± 5[a]	28 ± 7	68 ± 7[a]
Femoral vein concentration (pmol/liter)	27 ± 4	248 ± 33[a]	29 ± 6	282 ± 28[a]
Delivery to leg (pmol/min · 100 ml leg)	0.10 ± 0.02	1.00 ± 0.13[a]	0.12 ± 0.04	1.03 ± 0.16[a]
Glucose				
Arterial concentration (mmol/liter)	4.9 ± 0.1	4.9 ± 0.1	5.4 ± 0.1	5.1 ± 0.1
Leg uptake (μmol/min · 100 ml leg)	0.3 ± 0.2	2.3 ± 0.6[a]	0.4 ± 0.1	3.5 ± 0.8[a]
Endogenous production (μmol/kg · min)	9.9 ± 0.8	7.1 ± 0.4[a]	10.3 ± 0.5	7.6 ± 0.2[a]
Whole-body uptake (μmol/kg · min)	9.9 ± 0.8	14.4 ± 1.3[a]	10.3 ± 0.5	17.0 ± 1.1[a]

Values are the mean ± SE.

[a] $P < 0.05$ *vs.* baseline.

sulin infusion, Akt^{Ser473} phosphorylation increased significantly from baseline ($P < 0.05$) in both groups, with no differences between groups. A similar pattern was observed for Akt^{Thr308}, whereas $TSC2^{Thr1462}$ phosphorylation did not change significantly in either group. $mTOR^{Ser2448}$ phosphorylation significantly increased from baseline with hyperinsulinemia only in the control group ($P < 0.05$). $S6K1^{Thr389}$ phosphorylation increased during insulin infusion in both groups ($P < 0.05$) but was larger in the control group than in L-NMMA at the end of the infusion ($P < 0.05$). $4E\text{-}BP1^{Thr37/46}$ phosphorylation increased significantly with insulin at biopsy 3 in the control group only ($P < 0.05$).

Mixed-muscle FSR (Fig. 4)

During insulin infusion, FSR increased significantly in the control group ($P < 0.05$) but did not change in the L-NMMA group.

Phenylalanine kinetics (Table 3)

During hyperinsulinemia, phenylalanine arterial, venous, and muscle concentrations slightly but significantly decreased ($P < 0.05$), whereas phenylalanine arterial, venous, and muscle enrichments increased significantly ($P < 0.05$), with no differences between groups. Phenylalanine delivery tended to increase ($P = 0.07$) in the control group (+16.0 ± 9.4%) but did not change in the L-NMMA group (−7.2 ± 6.9%). Conversely, phenylalanine output from the leg did not change in the control group but decreased significantly ($P < 0.05$) in the L-NMMA group. As a result, phenylalanine net balance increased significantly in both groups ($P < 0.05$) with no group differences, but opposite mechanisms underlay this effect. The Control group had a significant increase ($P < 0.05$) in phenylalanine utilization for protein synthesis, with no change in proteolysis. The L-NMMA group showed a significant decrease ($P < 0.05$) in phenylalanine release from muscle, with no change in utilization for protein synthesis.

Discussion

Our results provide a first mechanistic demonstration that the endothelial-dependent increase in blood flow and muscle perfusion is a fundamental mechanism by which insulin stimulates skeletal muscle protein synthesis in young, healthy subjects. Our novel data indicate that insulin-stimulated vasodilation promotes muscle protein synthesis by increasing nutritive flow and, consequently, mTORC1 signaling, whereas Akt/PKB signaling is either not directly involved or only facilitates the process.

Specifically, local hyperinsulinemia at physiological postprandial levels induced significant increase in leg blood flow (10, 12) and muscle perfusion (17), enhancing Akt and mTORC1 signaling while also increasing skeletal muscle protein synthesis, resulting in an overall net anabolic effect. Conversely, administration of the eNOS inhibitor L-NMMA during local insulin infusion prevented the insulin-induced increase in blood flow and muscle perfusion, resulting in decreased amino acid delivery to the muscle, reduced mTORC1 signaling, and complete obliteration of the insulin-stimulatory effect on muscle protein synthesis. Interestingly, L-NMMA infusion did not prevent Akt signaling and the net muscle protein anabolic effect of insulin. However, the insulin's anabolic effect with L-NMMA was due to inhibition of proteolysis rather than an increase in synthesis.

Our findings that insulin enhances blood flow and microvascular recruitment, which can be blocked by L-NMMA, are consistent with previous reports (14, 20, 29–31). In our experiment, microvascular perfusion underwent a greater relative increase than total blood flow. This is in agreement with a previous report that the insulin effect on

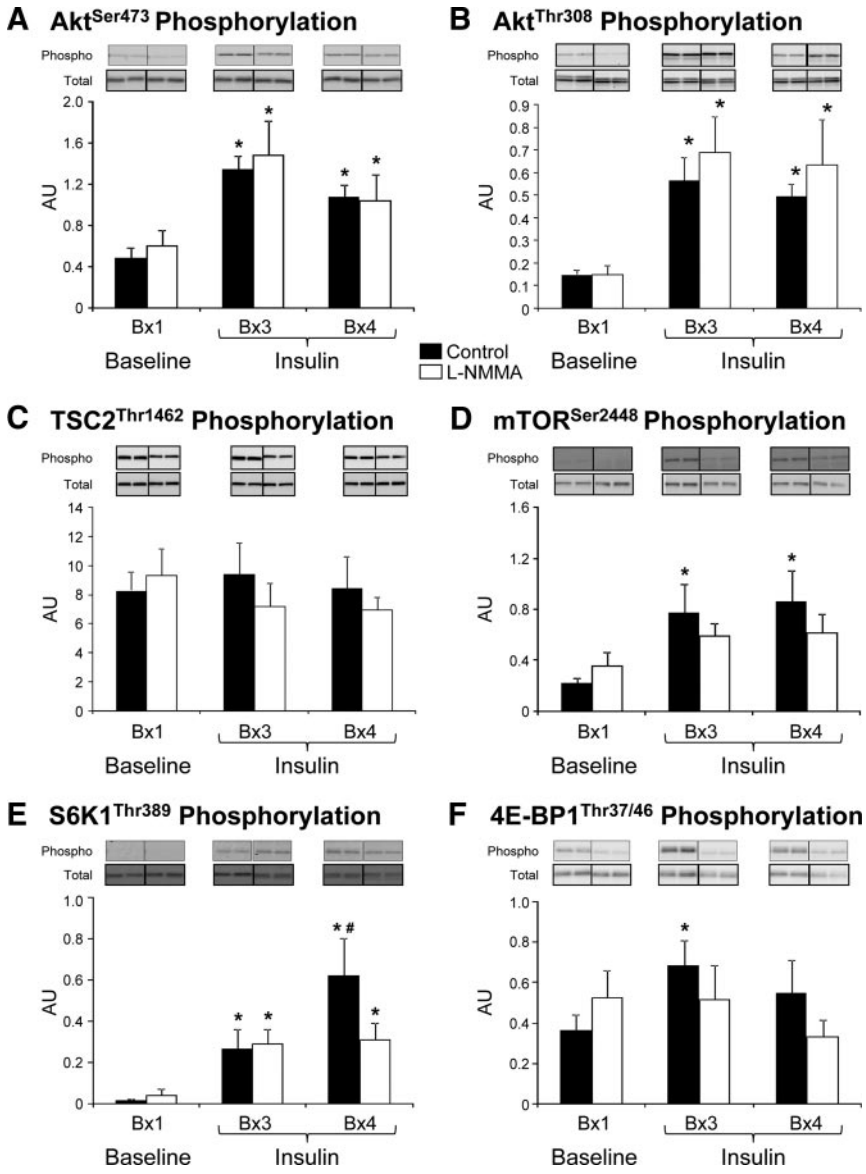

FIG. 3. Phosphorylation of Akt^{Ser473} (A), Akt^{Thr308} (B), TSC2^{Thr1462} (C), mTOR^{Ser2448} (D), S6K1^{Thr389} (E), and 4E-BP1$^{Thr37/46}$ (F) in the skeletal muscle of two groups of healthy young subjects at baseline (biopsy 1 at 120 min, Bx1), and during local insulin infusion (biopsy 3 at 330 min, Bx3; and biopsy 4 at 420 min, Bx4) in one leg with (L-NMMA, n = 7) or without (control, n = 7) concomitant infusion of the eNOS inhibitor L-NMMA. Blots for phosphorylated and total proteins are from a single representative control and L-NMMA subject, respectively. Data are the mean ± SE. *, $P < 0.05$ *vs.* baseline; #, $P < 0.05$ *vs.* control. AU, Arbitrary units.

microvasculature precedes and is not necessarily associated with changes in total blood flow (17). Besides stimulating vasodilation directly, nitric oxide synthesis through eNOS activation reduces production of the potent vasoconstrictor endothelin-1 (32), which is typically elevated in conditions associated with endothelial dysfunction, such as aging and insulin resistance (18, 33). We observed significantly lower endothelin-1 concentrations during isolated hyperinsulinemia, whereas administration of L-NMMA with insulin prevented this effect, mimicking the endothelial dysfunction of aging (12, 18).

An exciting finding of our study is that L-NMMA inhibition of insulin-induced vasodilation did not prevent the physiological increase in skeletal muscle Akt/PKB phosphorylation and glucose uptake, whereas it blunted mTORC1 signaling and protein synthesis. These results have several implications. Recent studies *in vitro* have shown that to reach the target tissues, insulin must first stimulate its own transport across the endothelium. This process requires an intact insulin signaling apparatus (34, 35). Although we did not directly measure insulin endothelial transport, our data suggest that eNOS activation and nitric oxide production are not involved in insulin transport across the endothelium, because the same insulin dose given alone or with L-NMMA induced similar increases in skeletal muscle Akt/PKB phosphorylation. While animal data have shown that inhibition of vasodilation during hyperinsulinemia can blunt the early muscle response of Akt/PKB and glucose uptake (31), our results indicate that endothelial-dependent vasodilation is not an essential contributor to muscle Akt/PKB signaling and glucose uptake in the later phases of hyperinsulinemia (1.5–3 h). Furthermore, a positive effect of insulin-induced vasodilation on glucose metabolism is more evident at higher glucose uptake levels than that achieved in our study, when increased perfusion and flow provide more uniform tissue exposure to glucose and reduce the artery-to-vein glucose gradient (14, 29, 31).

Conversely, our data clearly prove that the insulin-induced increase in mTORC1 signaling relies upon the hormone's effects on nutritive flow, which increases both nutrient delivery and the amount of muscle tissue exposed to circulating nutrients. Increased amino acid availability has been reported to stimulate mTOR phosphorylation independent of Akt/PKB phosphorylation (19, 36). Although the exact mechanisms underlying the ability of amino acids to regulate mTORC1 phosphorylation are not completely understood, the ability of amino acids to regulate the interaction of Rheb GTP with the mTOR complex may play a pivotal role because the binding of Rheb to mTOR appears to be necessary for mTORC1 activation (37, 38).

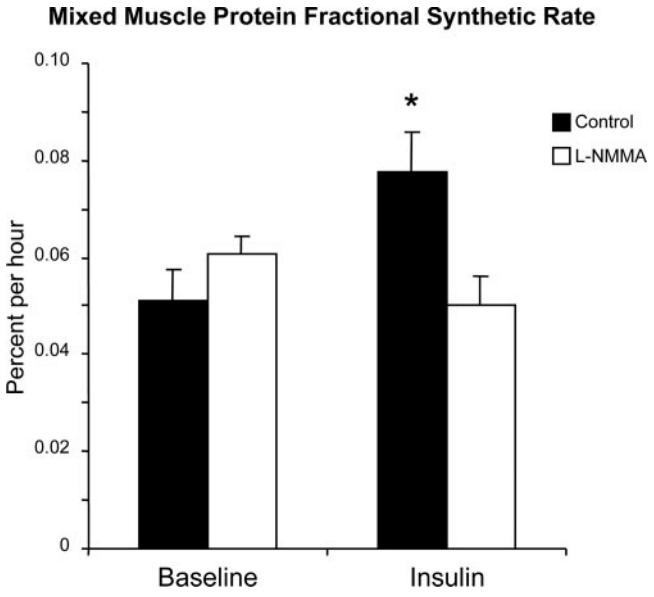

FIG. 4. Skeletal muscle mixed protein FSR in two groups of healthy young subjects at baseline and during local insulin infusion in one leg with (L-NMMA) or without (control) concomitant infusion of the eNOS inhibitor L-NMMA. Data are the mean ± SE. *, $P < 0.05$ *vs.* baseline.

Thus, the observed increases in $mTOR^{Ser2448}$, $S6K1^{Thr389}$, and $4E\text{-}BP1^{Thr37/46}$ phosphorylation and muscle protein synthesis in our control group likely resulted from the blood flow-mediated increase in amino acid delivery, a phenomenon that did not occur in the L-NMMA group. Because Akt/PKB can also phosphorylate mTORC1 (19), it might have exerted a facilitating effect on mTORC1 signaling and protein synthesis. However, phosphorylation of $TSC2^{Thr1462}$, a mTORC1 inhibitor that can be directly phosphorylated and inactivated by Akt (39, 40), did not change in either group, suggesting that Akt played a minor role under these experimental conditions. Akt^{Ser473} and Akt^{Thr308} data also suggest that upstream signaling through phosphatidylinositol 3-kinase and phosphoinositide-dependent kinase 1 was not different between the two groups (41), allowing us to exclude a significant role of phosphoinositide-dependent kinase 1 on mTORC1 signaling (42). The slight discrepancies between $mTOR^{Ser2448}$, $S6K1^{Thr389}$, and $4E\text{-}BP1^{Thr37/46}$ phosphorylation patterns could be due to the fact that the phosphorylation status at one site does not always predict mTOR activity or that we missed the peak of $mTOR^{Ser2448}$ phosphorylation due to the timing of the muscle biopsies. Regardless, mTOR activity increased in both groups, but more so in the control group as shown by the increased phosphorylation of its primary downstream effector, S6K1. We have also reported an alternate, differential mTOR regulation of 4E-BP1 and S6K1 phosphorylation in humans during exercise (26), which is analogous to the current findings. These results also suggest that our findings are unlikely due to a direct effect of L-NMMA on skeletal muscle cell signaling. It was recently shown in myotubes that NOS blockade by L-NMMA prevents the nitric oxide-induced attenuation of mTOR signaling and downstream translation (43). If L-NMMA had a direct effect on muscle, it should have enhanced, rather than blocked, mTOR phosphorylation and protein synthesis. In the L-NMMA group, prevention of the insulin-induced increase in nutritive flow and amino acid delivery perhaps outweighed any direct effect of nitric oxide availability on mTORC1 signaling. However, this area war-

TABLE 3. Leg free phenylalanine concentrations, enrichments, and kinetics in two groups of healthy young subjects at baseline and during local insulin infusion in one leg with (L-NMMA) or without (control) concomitant infusion of the eNOS inhibitor L-NMMA

	Control		L-NMMA	
	Baseline	Insulin	Baseline	Insulin
Phenylalanine concentration (μmol/liter)				
Femoral artery	59 ± 3	56 ± 3[a]	60 ± 4	58 ± 3[a]
Femoral vein	63 ± 3	55 ± 3[a]	65 ± 4	57 ± 3[a]
Muscle	72 ± 5	62 ± 4[a]	77 ± 8	66 ± 4[a]
Phenylalanine enrichment (tracer/tracee, %)				
Femoral artery	7.9 ± 0.3	9.0 ± 0.5[a]	7.6 ± 0.3	8.3 ± 0.4[a]
Femoral vein	6.4 ± 0.3	7.6 ± 0.3[a]	6.0 ± 0.6	6.7 ± 0.3[a]
Muscle	5.6 ± 0.2	6.5 ± 0.4[a]	5.0 ± 0.2	6.0 ± 0.2[a]
Phenylalanine kinetics (nmol/min · 100 ml leg)				
Net balance	-14 ± 3	3 ± 3[a]	−15 ± 2	4 ± 3[a]
Delivery to the leg	211 ± 30	240 ± 31[b]	217 ± 24	202 ± 29
Output from the leg	225 ± 31	237 ± 34	232 ± 25	198 ± 27[a]
Leg rate of appearance	49 ± 8	44 ± 9	58 ± 5	46 ± 4[a]
Leg rate of disappearance	35 ± 7	47 ± 7[a]	43 ± 5	51 ± 7
Release from proteolysis	55 ± 9	54 ± 11	66 ± 7	52 ± 5[a]
Utilization for protein synthesis	40 ± 8	56 ± 10[a]	51 ± 7	56 ± 8

Values are the mean ± SE.

[a] $P < 0.05$ *vs.* baseline.

[b] $P = 0.07$ *vs.* baseline.

rants further investigations. Finally, L-NMMA is not eNOS specific and could interfere with muscle contraction via inhibition of nNOS (44). Additionally, L-NMMA attenuates exercise-induced vasodilation (45), reducing the anabolic effect of exercise. However, our experiments were performed at rest, making it unlikely that these mechanisms were responsible for our findings. Collectively, these data suggest that insulin-induced increases in blood flow, microvascular flow, and amino acid delivery are key, interconnected, components of insulin's anabolic properties on skeletal muscle proteins.

The notion that insulin stimulates skeletal muscle protein synthesis in adult humans has long been debated because some studies reported that insulin administration was unable to stimulate muscle protein synthesis while it decreased protein breakdown (8, 9, 21), whereas several others reported an increase in protein synthesis with no change in breakdown (6, 46–48). We have previously discussed this issue at length (10–12, 18), suggesting that differences in vasodilation and amino acid delivery might have explained these discrepancies. Studies reporting reduced proteolysis with no change in protein synthesis employed systemic insulin administration in the absence of exogenous amino acid administration, resulting in decreased amino acid concentration and delivery (9, 21, 49). Conversely, studies reporting increased protein synthesis prevented hypoaminoacidemia using local insulin administration (as in the present study) or systemic infusion with amino acid coinfusion (6, 46–48, 50). The present study provides the mechanistic proof that our original hypothesis is correct, showing not only that blockade of insulin-induced vasodilation prevents the increase in protein synthesis but also that when this occurs in a subject with an otherwise intact insulin signaling apparatus, proteolysis decreases with a consequent protein-sparing effect. This finding does not appear to be an artifact of the mathematical models employed to calculate protein breakdown because both the two- and the three-pool models provided qualitatively comparable results. We can only speculate on the basic mechanisms underlying these opposite responses of muscle protein breakdown to hyperinsulinemia. It has clearly been shown that insulin activation of Akt/PKB inhibits protein breakdown probably via FOXO-mediated down-regulation of ubiquitin-proteasome activity (51, 52). However, this effect may be prevented when there is a concurrent increase in amino acid availability to the muscle tissue. This increase in nutritive flow may directly activate mTORC1 signaling (rather than mTORC2) because mTORC2 activation appears to be an essential component of the Akt-FOXO pathway (53). We cannot definitively determine from our data what cellular mechanisms are regulating these opposite responses of muscle protein breakdown to hyperinsulinemia, but future studies should examine the role of both mTOR complexes in the control of muscle protein turnover.

In summary, this is the first study to mechanistically demonstrate that insulin stimulates muscle protein synthesis not through Akt/PKB signaling but through increases in capillary recruitment, nutritive flow, and mTORC1 signaling. It also underscores that although insulin exerts a protein-sparing effect on the skeletal muscle of young individuals with normal insulin sensitivity, the mechanism is dependent on its ability to stimulate muscle perfusion. Further studies are needed to determine the mechanisms by which insulin controls skeletal muscle protein breakdown in relation to nutritive flow and whether endogenous meal-stimulated hyperinsulinemia acts through similar mechanisms to stimulate skeletal muscle protein synthesis.

Acknowledgments

We thank the study subjects for their participation, Ming Zheng and Shelley Medina for superb technical assistance, Francisco Pasdar-Shirazi for his assistance with Western blots, and the nurses and personnel of the University of Texas Medical Branch Clinical Research Center for their assistance in the clinical conduct of this study.

Address all correspondence and requests for reprints to: Elena Volpi, M.D., Ph.D., University of Texas Medical Branch, 301 University Boulevard, Galveston, Texas 77555-0460. E-mail: evolpi@utmb.edu.

This work was supported by National Institutes of Health Grants R01 AG18311, P30 AG024832, S10 RR16650, T32 HD07539, M01 RR00073, and UL1 RR029876.

Disclosure Summary: The authors report no conflict of interest.

References

1. **Kimball SR, Jefferson LS, Fadden P, Haystead TA, Lawrence Jr JC** 1996 Insulin and diabetes cause reciprocal changes in the association of eIF-4E and PHAS-I in rat skeletal muscle. Am J Physiol 270(2 Pt 1):C705–C709
2. **Kimball SR, Jurasinski CV, Lawrence Jr JC, Jefferson LS** 1997 Insulin stimulates protein synthesis in skeletal muscle by enhancing the association of eIF-4E and eIF-4G. Am J Physiol 272(2 Pt 1):C754–C759
3. **O'Connor PM, Bush JA, Suryawan A, Nguyen HV, Davis TA** 2003 Insulin and amino acids independently stimulate skeletal muscle protein synthesis in neonatal pigs. Am J Physiol Endocrinol Metab 284:E110–E119
4. **Suryawan A, O'Connor PM, Bush JA, Nguyen HV, Davis TA** 2009 Differential regulation of protein synthesis by amino acids and insulin in peripheral and visceral tissues of neonatal pigs. Amino Acids 37:97–104
5. **Bennet WM, Rennie MJ** 1991 Protein anabolic actions of insulin in the human body. Diabet Med 8:199–207

6. **Biolo G, Declan Fleming RY, Wolfe RR** 1995 Physiologic hyperinsulinemia stimulates protein synthesis and enhances transport of selected amino acids in human skeletal muscle. J Clin Invest 95:811–819
7. **Denne SC, Liechty EA, Liu YM, Brechtel G, Baron AD** 1991 Proteolysis in skeletal muscle and whole body in response to euglycemic hyperinsulinemia in normal adults. Am J Physiol 261(6 Pt 1):E809–E814
8. **Heslin MJ, Newman E, Wolf RF, Pisters PW, Brennan MF** 1992 Effect of hyperinsulinemia on whole body and skeletal muscle leucine carbon kinetics in humans. Am J Physiol 262(6 Pt 1):E911–E918
9. **Moller-Loswick AC, Zachrisson H, Hyltander A, Korner U, Matthews DE, Lundholm K** 1994 Insulin selectively attenuates breakdown of nonmyofibrillar proteins in peripheral tissues of normal men. Am J Physiol 266(4 Pt 1):E645–E652
10. **Fujita S, Rasmussen BB, Cadenas JG, Grady JJ, Volpi E** 2006 Effect of insulin on human skeletal muscle protein synthesis is modulated by insulin-induced changes in muscle blood flow and amino acid availability. Am J Physiol Endocrinol Metab 291:E745–E754
11. **Fujita S, Glynn EL, Timmerman KL, Rasmussen BB, Volpi E** 2009 Supraphysiological hyperinsulinaemia is necessary to stimulate skeletal muscle protein anabolism in older adults: evidence of a true age-related insulin resistance of muscle protein metabolism. Diabetologia 52:1889–1898
12. **Rasmussen BB, Fujita S, Wolfe RR, Mittendorfer B, Roy M, Rowe VL, Volpi E** 2006 Insulin resistance of muscle protein metabolism in aging. FASEB J 20:768–769
13. **Proud CG** 2002 Regulation of mammalian translation factors by nutrients. Eur J Biochem 269:5338–5349
14. **Baron AD, Tarshoby M, Hook G, Lazaridis EN, Cronin J, Johnson A, Steinberg HO** 2000 Interaction between insulin sensitivity and muscle perfusion on glucose uptake in human skeletal muscle: evidence for capillary recruitment. Diabetes 49:768–774
15. **Meneilly GS, Elliot T, Bryer-Ash M, Floras JS** 1995 Insulin-mediated increase in blood flow is impaired in the elderly. J Clin Endocrinol Metab 80:1899–1903
16. **Tack CJ, Schefman AE, Willems JL, Thien T, Lutterman JA, Smits P** 1996 Direct vasodilator effects of physiological hyperinsulinaemia in human skeletal muscle. Eur J Clin Invest 26:772–778
17. **Vincent MA, Dawson D, Clark AD, Lindner JR, Rattigan S, Clark MG, Barrett EJ** 2002 Skeletal muscle microvascular recruitment by physiological hyperinsulinemia precedes increases in total blood flow. Diabetes 51:42–48
18. **Fujita S, Rasmussen BB, Cadenas JG, Drummond MJ, Glynn EL, Sattler FR, Volpi E** 2007 Aerobic exercise overcomes the age-related insulin resistance of muscle protein metabolism by improving endothelial function and Akt/mammalian target of rapamycin signaling. Diabetes 56:1615–1622
19. **Hara K, Yonezawa K, Weng QP, Kozlowski MT, Belham C, Avruch J** 1998 Amino acid sufficiency and mTOR regulate p70 S6 kinase and eIF-4E BP1 through a common effector mechanism. J Biol Chem 273:14484–14494
20. **Vincent MA, Barrett EJ, Lindner JR, Clark MG, Rattigan S** 2003 Inhibiting NOS blocks microvascular recruitment and blunts muscle glucose uptake in response to insulin. Am J Physiol Endocrinol Metab 285:E123–E129
21. **Nygren J, Nair KS** 2003 Differential regulation of protein dynamics in splanchnic and skeletal muscle beds by insulin and amino acids in healthy human subjects. Diabetes 52:1377–1385
22. **Jorfeldt L, Wahren J** 1971 Leg blood flow during exercise in man. Clin Sci 41:459–473
23. **Vincent MA, Clerk LH, Lindner JR, Price WJ, Jahn LA, Leong-Poi H, Barrett EJ** 2006 Mixed meal and light exercise each recruit muscle capillaries in healthy humans. Am J Physiol Endocrinol Metab 290: E1191–E1197
24. **Wei K, Jayaweera AR, Firoozan S, Linka A, Skyba DM, Kaul S** 1998 Quantification of myocardial blood flow with ultrasound-induced destruction of microbubbles administered as a constant venous infusion. Circulation 97:473–483
25. **Clerk LH, Vincent MA, Jahn LA, Liu Z, Lindner JR, Barrett EJ** 2006 Obesity blunts insulin-mediated microvascular recruitment in human forearm muscle. Diabetes 55:1436–1442
26. **Dreyer HC, Fujita S, Cadenas JG, Chinkes DL, Volpi E, Rasmussen BB** 2006 Resistance exercise increases AMPK activity and reduces 4E-BP1 phosphorylation and protein synthesis in human skeletal muscle. J Physiol 576(Pt 2):613–624
27. **Wolfe RR** 1992 Radioactive and stable isotope tracers in biomedicine. In: Principles and practice of kinetic analysis. New York: Wiley-Liss
28. **Wolfe RR, Chinkes DL** 2005 Isotope tracers in metabolic research. In: Principles and practice of kinetic analysis. 2nd ed. New York: Wiley-Liss
29. **Clerk LH, Vincent MA, Lindner JR, Clark MG, Rattigan S, Barrett EJ** 2004 The vasodilatory actions of insulin on resistance and terminal arterioles and their impact on muscle glucose uptake. Diabetes Metab Res Rev 20:3–12
30. **Vincent MA, Montagnani M, Quon MJ** 2003 Molecular and physiologic actions of insulin related to production of nitric oxide in vascular endothelium. Curr Diab Rep 3:279–288
31. **Vincent MA, Clerk LH, Lindner JR, Klibanov AL, Clark MG, Rattigan S, Barrett EJ** 2004 Microvascular recruitment is an early insulin effect that regulates skeletal muscle glucose uptake in vivo. Diabetes 53:1418–1423
32. **Kourembanas S, McQuillan LP, Leung GK, Faller DV** 1993 Nitric oxide regulates the expression of vasoconstrictors and growth factors by vascular endothelium under both normoxia and hypoxia. J Clin Invest 92:99–104
33. **Mather KJ, Mirzamohammadi B, Lteif A, Steinberg HO, Baron AD** 2002 Endothelin contributes to basal vascular tone and endothelial dysfunction in human obesity and type 2 diabetes. Diabetes 51: 3517–3523
34. **Wang H, Liu Z, Li G, Barrett EJ** 2006 The vascular endothelial cell mediates insulin transport into skeletal muscle. Am J Physiol Endocrinol Metab 291:E323–E332
35. **Wang H, Wang AX, Liu Z, Barrett EJ** 2008 Insulin signaling stimulates insulin transport by bovine aortic endothelial cells. Diabetes 57:540–547
36. **Roccio M, Bos JL, Zwartkruis FJ** 2006 Regulation of the small GTPase Rheb by amino acids. Oncogene 25:657–664
37. **Long X, Lin Y, Ortiz-Vega S, Yonezawa K, Avruch J** 2005 Rheb binds and regulates the mTOR kinase. Curr Biol 15:702–713
38. **Long X, Ortiz-Vega S, Lin Y, Avruch J** 2005 Rheb binding to mammalian target of rapamycin (mTOR) is regulated by amino acid sufficiency. J Biol Chem 280:23433–23436
39. **Manning BD, Tee AR, Logsdon MN, Blenis J, Cantley LC** 2002 Identification of the tuberous sclerosis complex-2 tumor suppressor gene product tuberin as a target of the phosphoinositide 3-kinase/akt pathway. Mol Cell 10:151–162
40. **Inoki K, Li Y, Zhu T, Wu J, Guan KL** 2002 TSC2 is phosphorylated and inhibited by Akt and suppresses mTOR signalling. Nat Cell Biol 4:648–657
41. **Alessi DR, Andjelkovic M, Caudwell B, Cron P, Morrice N, Cohen P, Hemmings BA** 1996 Mechanism of activation of protein kinase B by insulin and IGF-1. EMBO J 15:6541–6551
42. **Vasudevan KM, Barbie DA, Davies MA, Rabinovsky R, McNear CJ, Kim JJ, Hennessy BT, Tseng H, Pochanard P, Kim SY, Dunn IF, Schinzel AC, Sandy P, Hoersch S, Sheng Q, Gupta PB, Boehm JS, Reiling JH, Silver S, Lu Y, Stemke-Hale K, Dutta B, Joy C, Sahin AA, Gonzalez-Angulo AM, Lluch A, Rameh LE, Jacks T, Root DE, Lander ES, Mills GB, Hahn WC, Sellers WR, Garraway LA** 2009 AKT-independent signaling downstream of oncogenic PIK3CA mutations in human cancer. Cancer Cell 16:21–32
43. **Frost RA, Nystrom GJ, Lang CH** 2009 Endotoxin and interferon-γ

inhibit translation in skeletal muscle cells by stimulating nitric oxide synthase activity. Shock 32:416–426
44. **Percival JM, Anderson KN, Huang P, Adams ME, Froehner SC** 2010 Golgi and sarcolemmal neuronal NOS differentially regulate contraction-induced fatigue and vasoconstriction in exercising mouse skeletal muscle. J Clin Invest 120:816–826
45. **Casey DP, Joyner MJ** 2009 NOS inhibition blunts and delays the compensatory dilation in hypoperfused contracting human muscles. J Appl Physiol 107:1685–1692
46. **Hillier TA, Fryburg DA, Jahn LA, Barrett EJ** 1998 Extreme hyperinsulinemia unmasks insulin's effect to stimulate protein synthesis in the human forearm. Am J Physiol 274(6 Pt 1):E1067–E1074
47. **Newman E, Heslin MJ, Wolf RF, Pisters PW, Brennan MF** 1994 The effect of systemic hyperinsulinemia with concomitant amino acid infusion on skeletal muscle protein turnover in the human forearm. Metabolism 43:70–78
48. **Wolf RF, Heslin MJ, Newman E, Pearlstone DB, Gonenne A, Brennan MF** 1992 Growth hormone and insulin combine to improve whole-body and skeletal muscle protein kinetics. Surgery 112:284–291; discussion 291–292
49. **Tessari P, Inchiostro S, Biolo G, Vincenti E, Sabadin L** 1991 Effects of acute systemic hyperinsulinemia on forearm muscle proteolysis in healthy man. J Clin Invest 88:27–33
50. **Bennet WM, Connacher AA, Scrimgeour CM, Jung RT, Rennie MJ** 1990 Euglycemic hyperinsulinemia augments amino acid uptake by human leg tissues during hyperaminoacidemia. Am J Physiol 259(2 Pt 1):E185–E194
51. **Gross DN, Wan M, Birnbaum MJ** 2009 The role of FOXO in the regulation of metabolism. Curr Diab Rep 9:208–214
52. **Sandri M** 2008 Signaling in muscle atrophy and hypertrophy. Physiology 23:160–170
53. **Guertin DA, Stevens DM, Thoreen CC, Burds AA, Kalaany NY, Moffat J, Brown M, Fitzgerald KJ, Sabatini DM** 2006 Ablation in mice of the mTORC components raptor, rictor, or mLST8 reveals that mTORC2 is required for signaling to Akt-FOXO and PKCα, but not S6K1. Dev Cell 11:859–871